# RSC Advances

## RSC Advances

www.rsc.org/advances

ROYAL SOCIETY OF CHEMISTRY

www.rsc.org/advances

# Journal Name

**ARTICLE TYPE**

# Water-soluble Gold Nanoclusters with pH-dependent Fluorescence and High Colloidal Stability over a Wide pH Range via Co-reduction of Glutathione and Citrate

**Wenchao Ding,**[a] **Yong Liu,**[a] **Yijing Li,**[a] **Qiurong Shi,**[a] **Houshen Li,**[a] **Haibing Xia,\***[a] **Dayang Wang**[b] **and**

5 **Xutang Tao**[a]

We present a strategy for synthesis of water-soluble, monodisperse, highly fluorescent gold nanoclusters (Au NCs) with size of 1.8 nm by co-reduction of glutathione and citrate (denoted as GS/C-Au NCs) for
10 24 h at 50 °C. The high content of Au(I)−thiolate complexes (about 75 %) on the surfaces of core-shell structured GS/C-Au NCs is responsible for their strong fluorescence generated by the aggregation-induced emission (AIE). The advantages of this method by using citrate are as follows: (i) lower the reaction temperature; (ii) control formation rate of Au(0) cores by selective reduction of Au(III) ions; and (iii) enhance the colloidal stability of GS/C−Au NCs in the wide pH range from 4.1 to 8.6 due to
15 differently stable states of glutathione-citrate complex on the surfaces. In addition, fluorescence intensity of GS/C−Au NCs obtained is pH-dependent and can be reversibly adjusted in the pH range from 4.1 to 8.6 due to changes in their surface charge density stemming from the transitions among differently stable states of glutathione-citrate complex. Our preliminary study also demonstrates that the resulting GS/C−Au NCs can be used as fluorescent nanoprobes in bio-imaging.

## 20 1. Introduction

Over the past decade, gold nanoclusters (Au NCs) with ultrasmall size (< 2 nm), consisting of several to tens of Au atoms,[1,2] have stimulated extensive interest due to their attractive superiority: ultimately small sizes, excellent biocompatibility, favorable
25 stability, and water solubility. Recently, fluorescent Au NCs are recognized as promising candidates for cell labeling,[3-8] biosensing,[9-11] and selective detection of trace metal ions, *e.g.* Ag(I), Cr(III), Pb(II), Hg(II) etc.[12-14] Among these Au NCs, thiol-protected Au NCs are emerging as promising supermolecules,[15,16]
30 which are chemically stable and exhibit bright fluorescence ranging from the visible to the infrared depending on the number of atoms of clusters.[17] In addition, glutathione (GSH) capped Au NCs are widely studied[18-22] because of the easy accessible synthetic availability, great biocompatibility, and facile further
35 surface functionalization for biological applications. It was reported in the previous studies that the GS−Au NCs prepared by using strong reductant, such as NaBH₄, emitted very faint fluorescence with a quantum yields in the range from $10^{-3}$ to $10^{-5}$ due to the formation of high ratio of big Au nanoparticles in
40 size.[12,19,23-25] Thus, mild reducing condition and slow reduction kinetics are pivotal consideration for preparation of high fluorescent Au NCs. For instance, the luminescent GS−Au NCs composed of Au(0) atoms and Au(I) atoms (40~50 %) were synthesized by the dissociation process of GSH−gold(I) polymers
45 directly in aqueous solution at room temperature for 2 weeks by

Zheng group.[26] The presence of high percentage of Au(I) atoms was responsible for the unique optical properties of the luminescent Au NCs. However, the origin of luminescence in thiolate-protected Au NCs is still not clear. More recently, Xie
50 group[18] developed one new strategy to prepare the luminescent core-shell structured Au(0)@Au(I)−thiolate NCs with a quantum yield of ~ 15 % by selective reduction of Au(I) by the disulfide group of the resultant GSSG for 24 h at high temperature (70 °C). It was proposed that the strong luminescence was generated by
55 the aggregation-induced emission (AIE) of Au(I)−thiolate complexes on the NC surfaces; GS−Au NCs were highly luminescent when the molar ratio of Au(I) in the compact shells to Au(0) atoms in the cores was about 3:1.

It is known that the structure and activity of molecules are
60 dependent on pKa values of ionizable groups in them. As suggested in literatures, the existing state of polymeric Au(I)−GS complexes in water is pH-dependent, which can be as solution (pH < 1.8 or pH > 5.3), gel (1.8 < pH < 2.4) or suspension (2.4 < pH < 5.3).[27] Consequently, the stability of Au NCs with GS
65 ligand solely also would be pH-dependent, thus limiting their application in cell due to formation of gel or suspension as the pH range in the human cell is between 4 and 7.5. Therefore, the additional ligand is necessary to improve their colloidal stability and maintain their high luminescence at the same time.
70 Meanwhile, citrate is also extensively used as a reducing agent for synthesis of noble metal NCs.[28-30] It is well-known for its simple and safe operation, its negligible toxicity and its ease with ligand exchange. More importantly, citrate is a good buffer and

can associate with GSH by formation of bonds between carboxylate groups and positive amino groups. Thus, the use of citrate for stabilization of Au NCs may enhance their colloidal stability.

Herein, we present a strategy for synthesis of water-soluble, monodisperse, highly fluorescent Au NCs with size of 1.8 nm by co-reduction of GSH and citrate for 24 h at 50 °C. The advantages of this method by using citrate are as follows: (i) lower the reaction temperature; (ii) control formation rate of Au(0) cores by selective reduction of Au(III) ions; and (iii) enhance the colloidal stability of GS/C−Au NCs in the wide pH range from 4.1 to 8.6 due to different stable states of glutathione-citrate complex on the surfaces. In addition, fluorescence intensity of GS/C−Au NCs obtained is pH-dependent and can be reversibly adjusted in the pH range from 4.1 to 8.6 due to changes in their surface charge density stemming from the transitions among differently stable states of glutathione-citrate complex. Our preliminary study also demonstrates that the resulting GS/C−Au NCs can be used as fluorescent nanoprobes in bio-imaging.

## 2. Experimental

### 2.1 Chemicals.

All chemicals were commercially available and used without further purification. Chloroauric acid tetrahydrate ($HAuCl_4·4H_2O$), trisodium citrate dihydrate ($Na_3C_6H_5O_7·2H_2O$), sodium borohydride ($NaBH_4$) were purchased from Sinopharm Chemical Reagent Co. Ltd. Reduced glutathione (GSH) was purchased from Aladdin. The water used in all experiments was prepared in a three stage Millipore (A10) purification system and had a resistivity higher than 18.2 MΩ cm. The aqueous $HAuCl_4$ solution was prepared before use and stored in the fridge (+4 °C).

### 2.2 Synthesis of fluorescent GS/C−Au NCs.

A freshly prepared aqueous solution of GSH (0.3 ml, 50 mM) was mixed with $HAuCl_4$ (0.5 ml, 25 mM) aqueous solution at molar ratio of 1.2:1 at room temperature. The color of the resulting mixture turned from yellow to brown instantaneously, then to pale yellow in several seconds, implying the formation of GS−Au(I) complexes by GSH reduction. After mixing of about 3 min, 1.5 ml of citrate solution (50 mM) was added into the above mixture. The mixture obtained was then heated to 50 °C under stirring for about 24 h. The color of the mixture obtained gradually evolved from nearly colorless to bright-yellow, implying the formation of ultrasmall Au nanoclusters (GS/C−Au NCs). The final concentrations of GSH, citrate and $HAuCl_4$ were 6.5 mM, 32.6 mM and 5.4 mM, respectively. The products can be used without purification and stored at room temperature for 6 months with negligible changes in their optical properties.

### 2.3 Cell culture and staining.

HeLa cancer cells were cultured in Dulbecco's modified Eagle's medium (DMEM) supplemented with penicillin/streptomycin and 10 % bovine calf serum in a 5 % $CO_2$ incubator at 37 °C. Circular quartz coverslips (Leica Microsystems, Wetzlar, Germany) were incubated with 50 μg ml⁻¹ fibronectin in phosphate buffered saline (PBS, containing monobasic potassium, sodium chloride and dibasic sodium phosphate, Invitrogen) for 1 h, and HeLa cells were grown on the fibronectin-coated quartz coverslips overnight.

After removing the medium by three times washing with PBS, cells were incubated with GS/C−Au NCs solution (200 μg ml⁻¹) for 30 min. Cells were then washed thrice again with the same buffer solution and suspended in indicator free DMEM for imaging.

### 2.4 Wide-field fluorescence microscopy imaging.

Wide-field fluorescence microscopy images were acquired with an Olympus IX71 inverted microscope coupling with CCD and display controller software.

### 2.5 Materials characterization.

Transmission electron microscopy (TEM) and high-resolution transmission electron microscopy (HR-TEM) images were obtained with a JEOL JEM-2100F transmission electron microscope operating at an acceleration voltage of 200 kV. Dynamic Light Scattering (DLS) and zeta-potential analyses were performed at room temperature on a Malvern Zetasizer Nano ZS equipped with 50 mW 633 nm laser and a digital auto correlator with a scattering angle of 173° at 25 °C. The fluorescence spectra were obtained with a Hitachi F-4500 fluorescence spectrophotometer. UV-vis absorption spectroscopy was recorded on a Varian Cary 50 spectrophotometer, using 10 mm path length quartz cuvettes. X-Ray Photoelectron Spectroscopy (XPS) measurements were carried out on Thermo Fisher Scientific Escalab 250 XPS spectrometer, using Al Kα X-ray radiation for excitation. All spectra were referenced to the C1s peak at 284.6 eV.

## 3. Results and discussion

### 3.1 Synthesis of GS/C−Au NCs.

The synthetic strategy for synthesis of highly orange-emitting fluorescent GS/C−Au NCs is shown in Scheme 1. Firstly, the GSH solution was added into the aqueous $HAuCl_4$ solution at room temperature, in which the molar ratio of GSH to $HAuCl_4$ was 1.2:1 (Scheme 1a).
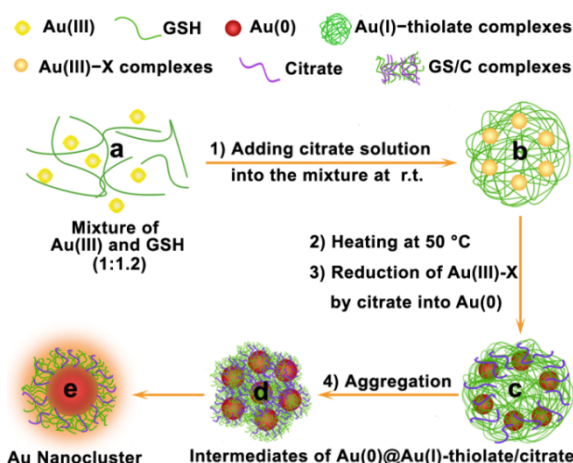


**Scheme 1** Schematic representation of synthetic strategy for synthesis of highly orange-emitting fluorescent Au(0)@Au(I)−GS/C Au NCs via selective reduction of Au(III)−X complexes by citrate at 50 °C.

The color of the resulting solution changed from yellow (belonging to the whole Au(III) ions before reduction) to brown instantaneously, and to pale yellow within 3 min. The distinct

color changes represent the formation of Au(I)−thiolate complexes (Scheme 1b) due to the reduction of partial Au(III) to Au(I) ions by GSH and the immediate coordination of Au(I) to the thiol group of GSH; the resulting solution with pale yellow indicates the presence of remaining Au(III) complexes due to partial reduction by insufficient GSH (Scheme 1b). This is reasonable as the Au(III) ions would be partially reduced[31-33] when the ratio of thiol to gold was smaller than 2. However, due to the strong absorption of Au(I)-thiolate complex, the presence of Au(III) ions cannot be detected by UV-vis method (Fig. S1A†) which are usually used in literatures.[28] However, the color of the mixed solution of GSH and HAuCl₄ at different molar ratio after 3 min is different, which can evidence the presence of Au(III) ions (Fig. S1B†). Au(I)−thiolate complexes (Scheme 1b) would be formed due to the strong binding [between Au(I) and S] in Au(I)−thiol; the strong affinity of thiol for Au(I) also protected the Au(I) oxidation state from further citrate reduction. In addition, remaining Au(III) ions would coordinate to the ligands (*e.g.* -COOH, -NH₂ and Cl⁻, denoted as X) in the mixture solution to form Au(III)−X complexes (Scheme 1b) as precursors for formation of Au cores.

Next, the citrate solution was added into the mixture mentioned above. The color of the reaction mixture slowly evolved into bright-yellow at 50 °C during 24 h. In this stage, Au(III)−X complexes, which were mainly composed of Au(III)−citrate complex after citrate addition, were reduced to Au(0) atoms by citrate at 50 °C. The *in situ* Au(0) atoms were subsequently segregated by Au(I)−thiolate complexes to form Au(0)-Au(I)-thiolate intermediates (Scheme 1c and 1d), due to the high affinity between Au(0) atoms and Au(I) ions.[34]

Eventually, the Au(I)−thiolate complexes and Au(0) atoms would slowly condense into a compact shell and a core, respectively, leading to the formation of core-shell structured GS/C protected Au@Au(I) NCs with orange-emitting fluorescence (Scheme 1e).

Unless pointed out specifically, the concentrations of GSH, citrate and HAuCl₄ used in this work for synthesis of as-prepared GS/C−Au NCs at 50 °C were 6.5 mM, 32.6 mM and 5.4 mM, respectively.

### 3.2. Fourier transform infrared (FT-IR) spectrum of GS/C−Au NCs.

In the Fourier transform infrared (FT-IR) spectrum of as-prepared GS/C Au NCs (Fig. S2a†), the peak at 3444 cm⁻¹ belongs to the O–H stretching vibration.[35] The peak of N–H stretching vibration at 3250 cm⁻¹ becomes rather weaker than that in GSH molecules (Fig. S2b†). The peak at 1538 cm⁻¹ is the characteristic band of −NH₃⁺. The peak at 1640 cm⁻¹ and 1387 cm⁻¹, corresponds to asymmetric stretching and symmetric stretching of carboxylate anion (–COO⁻), respectively. However, slight changes including the peak position, band shape and intensity are due to the interactions between –COO⁻ and −NH₃⁺.[35,36] These characteristic bands indicate the presence of the GHS and citrate ligands, in comparison with the FT-IR spectra of GHS and citrate ligands (Fig. S2b† and S2c†). The peak at 2524 cm⁻¹, which corresponds to stretching vibration of the sulfhydryl group (–SH) in GSH ligand, is not observed due to the binding of glutathione to the cluster surface.[37]

### 3.3 Photophysical Properties of GS/C−Au NCs.

The as-prepared GS/C−Au NCs show bright-yellow in solution and deep-yellow in powder state under visible light (Fig. 1A). However, they show bright orange-colored fluorescence in both solution and solid state under UV light (Fig. 1B), indicating that highly fluorescent Au NCs are obtained.
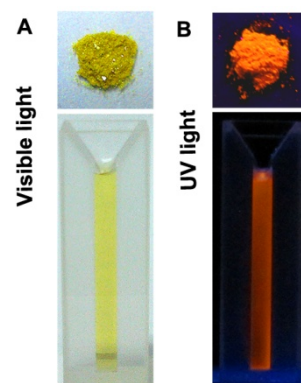


**Fig. 1** Digital photographs of as-prepared GS/C−Au NCs in the solid state (upper row) and in water (lower row) under visible light (A) and UV light (B).
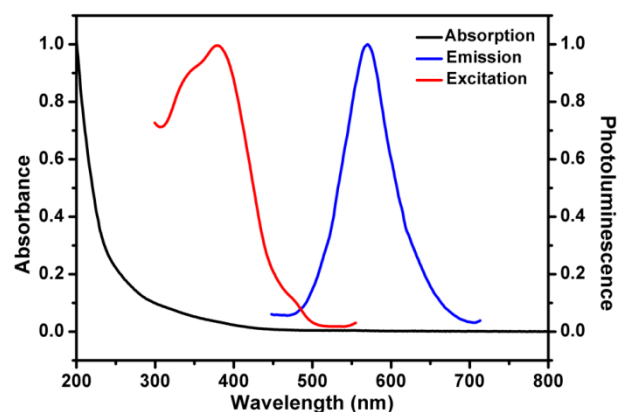


**Fig. 2** UV-vis absorption spectrum (black curve), fluorescence emission spectrum (blue curve, emission maximum at 575 nm), and excitation spectrum (red curve, excitation maximum at 385 nm) of the aqueous solution of as-prepared GS/C−Au NCs.

These GS/C−Au NCs exhibit an emission maximum at 575 nm and the excitation maximum is localized at 385 nm (blue and red curves in Fig. 2, respectively). The emission maximum is kept unchanged with the excitation wavelengths varying from 320 to 420 nm, indicating that there is single-component Au NCs with real fluorescence rather than mere light scattering (Fig. S3†).[7,14] Similar to the luminescent Au(I) complexes, GS/C−Au NCs obtained have a large Stokes shift of 190 nm. The emission from the aggregates of pure Au(I)−thiolate complexes is attributed to ligand-to-metal charge transfer (LMCT) or ligand-to-metal-metal charge transfer (LMMCT) from the sulfur atoms in the thiolates to the Au atoms and subsequent radiative relaxation.[18,38,39] In our cases, the presence of citrate ions and decreasing content of sulfur atoms in the aggregates of Au(I)−thiolate complexes weaken the charge transfer, and thus render the stoke shift smaller than that of pure Au(I)−thiolate complexes. Compared with the absorption spectra of larger Au nanoparticles, there is no any observed surface plasmon absorption for these fluorescent GS/C−Au NCs

(black curve in Fig. 2), illustrating that their size is rather smaller. The disappearance of surface plasmon absorption also suggests that some gold atoms are in high oxidation states and fail to provide free electrons.[26,40] Moreover, no molecular-like
[5] absorption of conventional thiolate-protected Au NCs with more than 15 Au atoms was observed (peaks at > 500 nm).[21,41,42]

The quantum yield (QY) of these GS/C−Au NCs in aqueous solution was measured to be 1.7 %, using rhodamine B (QY = 31 % in water) as the reference. Although the QY value is lower than
[10] for most organic dyes and protein-protected Au NCs, the fluorescence intensity is sufficient for their application as fluorescent probes in cellular imaging.[7] The higher quantum yield of pure Au(I)−thiolate-citrate complexes is attributed to their dense aggregation, which generate more intense luminescence
[15] because of their stronger aurophilic Au(I)···Au(I) interactions and more restrained molecular vibrations.[18] Thus, the introduction of citrate ions would weaken the intra- and inter-complex aurophilic Au(I)···Au(I) interactions and consequently decrease the fluorescence intensity of the complexes,[43-45] due to the formation
[20] of bonds between GSH and citrate ion. In our cases, luminescence intensity of as-prepared Au NCs can be improved by increasing pH of their solution to tune the aggregation states of Au(I)−thiolate complexes by breaking the bonds between citrate and GSH ligands.

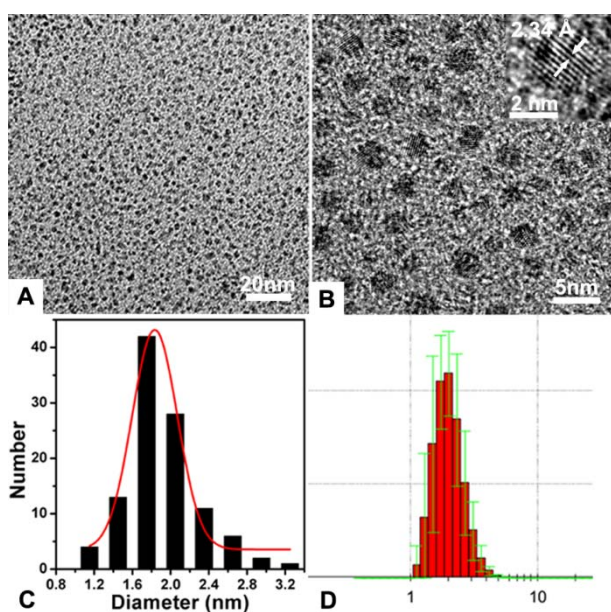[25] **3.4 Size characterization of GS/C−Au NCs.**



**Fig. 3** Typical TEM image (A) and HR-TEM image (B) of as-prepared GS/C−Au NCs. Histogram of the size distribution of GS/C−Au NCs obtained from analysis of counting 100 particles in TEM image (C) and
[30] from DLS results (D).

The size of GS/C−Au NCs is about $1.8 \pm 0.2$ nm, which is obtained from analysis of counting 100 individual particles in the typical TEM image (Fig. 3A and 3C). The as-prepared NCs were also well dispersed in water; no aggregates are observed on TEM
[35] image (Fig. 3A and 3B). The inset in the HR-TEM image (Fig. 3B) shows lattice planes separated by 2.34 Å, corresponding to the (111) lattice spacing (2.34 Å) of the face centred cubic Au.[46] In addition, the hydrodynamic diameter of the as-prepared GS/C−Au NCs is $2.0 \pm 0.3$ nm in the DLS measurement (Fig.

[40] 3D). Note that the slightly increase in size of the Au NCs obtained from DLS measurement is attributed to the fact that the GSH/citrate shells and solvent molecules both contribute to the hydrodynamic diameter. The small size makes the GS/C−Au NCs fascinating for the applications in high resolution molecular and
[45] cellular imaging research.[47, 48]

**3.5 X-ray photoelectron spectroscopy study of GS/C−Au NCs.**

To further confirm the valence states of gold in the GS/C−Au NCs, XPS was used to investigate the oxidation states of Au. The Au 4f XPS spectrum (Fig. 4A) reveals the binding energy (BE) of
[50] Au $4f_{7/2}$ and Au $4f_{5/2}$ at 84.3 eV and 88.0 eV, respectively. The Au $4f_{7/2}$ BE is located at 84.3 eV, which is higher than for bulk Au(0) (83.8 eV) and lower than for GS−Au(I) complexes (85 eV).[26] The Au 4f peak is then deconvoluted into Au(0) and Au(I) components with binding energies of 83.9 eV and 84.4 eV,
[55] respectively (Fig. 4B), which are in good agreement with those reported in the previous studies.[18,26] The XPS results strongly demonstrate the presence of Au(0) atoms and Au(I) in the fluorescent GS/C−Au NCs. As the intensities of Au $4f_{7/2}$ BE are dependent of the valence states, the molar ratio of Au(I) to Au(0)
[60] atoms in the fluorescent GS/C−Au NCs is about 3:1 according to deconvolution of the BE peak (Fig. 4B). The result confirms that the Au NCs obtained were composed of a small Au(0) core and GS/C−Au(I) complex shell.[18]
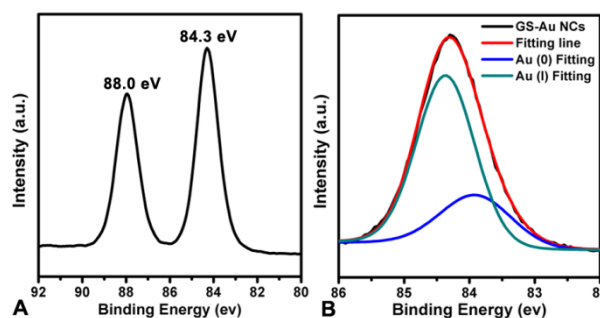


[65] **Fig. 4** Au 4f XPS spectrum of as-prepared GS/C−Au NCs showing the binding energy (BE) of Au $4f_{7/2}$ were 84.3 eV and 88.0 eV, respectively (A). After deconvolution of the BE peak of GS/C−Au NCs, two peaks at 83.9 eV and 84.4 eV were found, which were assigned to Au(0) and Au(I), respectively (B).

[70] **3.6 Influence of reaction parameters on fluorescence intensity of GS/C−Au NCs.**

GSH was used as the reducing-cum-protecting agent for formation of Au(I)−thiolate complexes. Its amount would determine the proportion of Au(I) at the first stage as RSH can
[75] totally reduce Au(III) into Au(I) ions with molar ratio of 2:1.[33] In addition, the remaining Au(III) ions were transformed into the Au(0) atoms by citrate reduction[28] to form the cores (Scheme S1). Therefore, the optimal ratio of GSH-to-HAuCl₄ in our case was 1.2:1, which is lower than that used by Xie group (1.5:1). In
[80] present case, about 60 % of Au(III) ions are reduced to Au(I) by GSH to Au(I)−thiolate complexes and about 40 % of Au(III) ions are remained, which is indicted by the pale yellow color of the resulting solution (b in Fig. S1B†).

Control experiments were carried out to investigate the
[85] influence of GSH-to-HAuCl₄ ratios. When the GSH-to-HAuCl₄ ratio increases to 1.4:1, more Au(III) ions are reduced to form

Au(I)−thiolate complex; fewer Au(III) ions are reduced to form Au(0) atoms accordingly. As expected, the solution of Au NCs obtained were pale yellow and emitted very low fluorescence (blue curve in Fig. 5A).
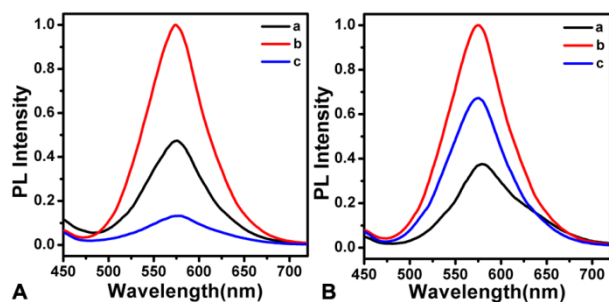


**Fig. 5** (A) Fluorescence emission spectra of GS/C−Au NCs obtained under different ratios of GSH-to-HAuCl₄: 1.0:1 (a, black curve), 1.2:1 (b, red curve) and 1.4:1 (c, blue curve). The concentrations of HAuCl₄ and citrate are 5.4 mM and 32.6 mM, respectively. The fluorescence intensity of as-prepared GS/C−Au NCs solution with GSH-to-HAuCl₄ of 1.2:1 was defined as 1. (B) Fluorescence emission spectra of GS/C−Au NCs obtained under different citrate concentrations: 10.9 mM (a, black curve), 32.6 mM (b, red curve), and 43.5 mM (c, blue curve). The concentrations of GSH and HAuCl₄ are 6.5 mM and 5.4 mM, respectively. The fluorescence intensity of as-prepared GS/C−Au NCs solution at citrate concentration of 32.6 mM was defined as 1.

Conversely, when GSH-to-HAuCl₄ ratio decreases to 1.0:1, fewer Au(III) ions are reduced to form Au(I)−thiolate complex by GSH reduction; more Au(III) ions are reduced to form Au(0) atoms by citrate reduction, which lead to the formation of byproducts (*e.g.* larger Au NPs, inset in Fig. S4†) in the solution of Au NCs obtained. It is also further confirmed by the UV-vis spectrum that there is one obvious peak of surface plasmon absorption of gold NPs at 550 nm (red curve in Fig. S4†). The solution of as-prepared Au NCs also has lower fluorescence intensity (black curve in Fig. 5A).

It is known that citrate plays multiple roles (such as reducing agent, capping agent and pH mediator) in the preparation of gold nanoparticles.[28,49,50] In our case, the optimal citrate concentration at 50 °C for reduction of the remaining Au(III) ions to Au(0) atoms is 32.6 mM. When the citrate concentration at 50 °C is 10.9 mM, the color of the final products obtained is dark yellow. The emission maximum shows obvious red-shift from 575 nm to 580 nm; the peak has a lower intensity and becomes broader and more asymmetric (black curve in Fig. 5B), in comparison with that of GS/C−Au NCs obtained under optimal citrate concentration. In addition, the TEM image shows that there are plenty of big agglomerations of Au NCs besides the GS/C−Au NCs in normal size (Fig. S5A†). The formation of big agglomerations of GS/C−Au NCs leads to the decrease in fluorescence intensity. This result also indicates that all of Au NCs cannot be stabilized at the citrate concentration of 10.9 mM (refer to the discussion later on colloidal stability) as the present amount of citrate is enough to totally reduce the Au(III) ions.

When the citrate concentration at 50 °C increases to 43.5 mM, the Au NCs obtained are still highly monodisperse. However, their size is about 1.5 nm in the TEM image and slightly smaller (Fig. S5B†), which is consistent with slight blue-shift of emission peak at 574 nm. The result indicates that high concentration of citrate would speed up the nucleation, thus leading to size

decrease. In our case, when the reaction is performed at 50 °C, this effect of the citrate concentration should be rationalized as a result of the deliberate balance of the stabilizing and reducing roles of the citrate. Either the stabilizing role of citrate weakened at a lower concentration or its reducing role strengthened at a higher concentration, has a side effect on the fluorescence intensity of Au NCs.

In our case, the Au(0) cores of GS/C−Au NCs are mainly formed by the reduction of Au(III)−X complexes by citrate, which rate is determined by citrate concentration and reaction temperature. Thus, the effect of reaction temperature on fluorescence intensity of Au NCs is also investigated at fixed citrate concentration. It is found that the fluorescence intensity is rather low when the reaction temperature is lower than 50 °C even after 24 h (Fig. 6), although it can reach the close fluorescence intensity after one week.
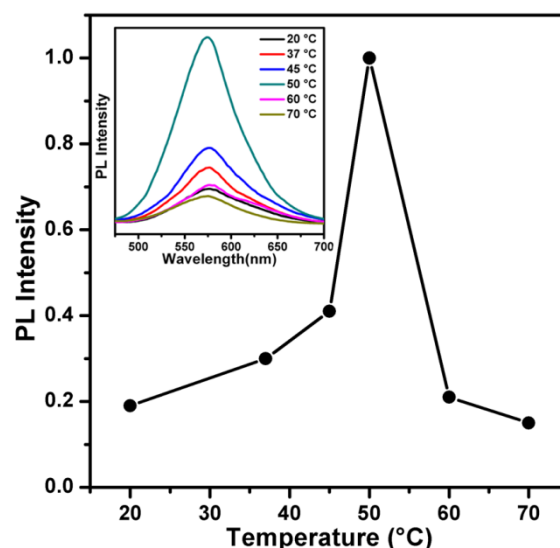


**Fig. 6** Fluorescence intensity of GS/C−Au NCs at extinction maximum of about 575 nm as a function of reaction temperature from 20 °C to 70 °C. The fluorescence intensity is normalized by that of the Au NCs solution obtained at 50 °C. The inset is the curves of the fluorescence emission spectra (excitation at 385 nm) of the Au NCs solution obtained at different reaction temperatures. The concentrations of GSH, citrate and HAuCl₄ used for all of sample are 6.5 mM, 32.6 mM and 5.4 mM, respectively.

However, the fluorescence intensity of Au NCs obtained under at 60 °C and 70 °C become rather low although the reaction time can be shorten to 6 h and 4 h, respectively. This may be due to the formation of large Au nanoparticles under high reaction temperature (Fig. S6†). The optimal reaction temperature (at about 50 °C) may meet the fast formation of Au(0) atoms while the Au(I)−GS/C complexes and Au(0) atoms have enough time to condense into the final product.

The time-evolution of formation process of GS/C−Au NCs at 50 °C was monitored by fluorescence emission spectra. As shown in Fig. 7, the Au NCs start to show fluorescence after 6 h, their fluorescence intensity then increases gradually over the following 16 h, and then levels off after 22 h eventually. Therefore, our present method is facile and complete within 24 h at lower temperature, making it promising for practical applications.
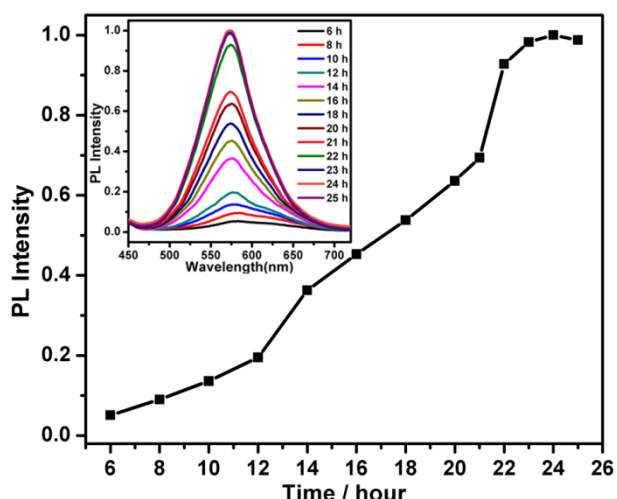
**Fig. 7** Fluorescence intensity of GS/C–Au NCs at 575 nm as a function of reaction times. The inset shows the time-dependent fluorescence emission spectra during the formation process (excitation at 385 nm). The fluorescence intensity of the as-prepared GS/C−Au NCs solution obtained at 24 h was defined as 1.

### 3.7 Influence of pH on colloidal stability of GS/C−Au NCs.
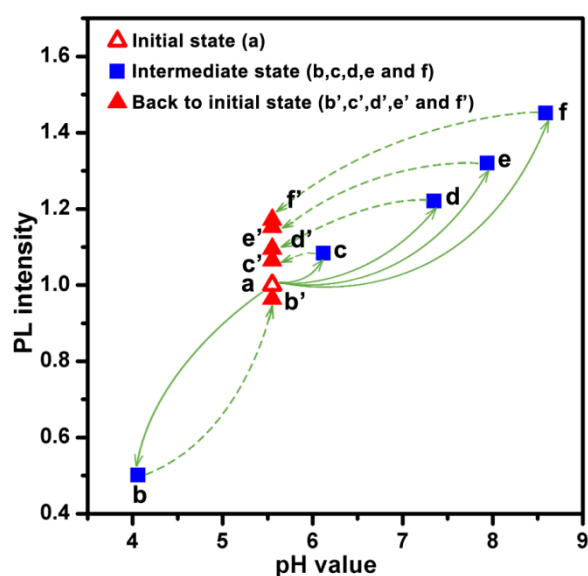


**Fig. 8** (Blue solid square) the plot of the fluorescence intensities of the GS/C−Au NCs solutions under the different pH values by addition of a certain volume of HCl (0.1 M) or NaOH (0.1 M) into the solution of as-prepared GS/C−Au NCs with an initial pH of about 5.6 (a, red open triangle): 4.1 (b), 6.1 (c), 7.4 (d), 7.9 (e), and 8.6 (f). (Red solid triangle) the plot of the fluorescence intensities of GS/C−Au NCs solutions with the recovered pH of about 5.6 by addition of a certain volume of HCl (0.1 M) or NaOH (0.1 M) into the GS/C−Au NCs solution with pH values of 4.1 (b to b'), 6.1 (c to c'), 7.4 (d to d'), 7.9 (e to e'), and 8.6 (f to f'). The initial pH of the aqueous solution of as-prepared GS/C−Au NCs is about 5.6 (a, red open triangle), at which their fluorescence intensity was defined as 1.

The structures of molecules with ionizable groups are dependent on the pKa values. The GSH molecule has four pKa values, which are 2.12, 3.53, 8.66 and 9.12, respectively. Thus, the environmental pH has an effect on the structures of GSH molecule (Fig. S7A†). Meanwhile, the citric acid has three pKa values, which are 3.13, 4.76, and 6.4, respectively (Fig. S7B†).

Depending on the environmental pH values, citric acid can evolve from dihydrogen citrate ($H_2Cit^-$) to hydrogen citrate ($HCit^{2-}$) or citrate ions ($Cit^{3-}$). Consequently, the carboxylate groups of citrate would associate with positive amino group of GSH molecules when the environmental pH is bigger than 3.13 ($pKa_1$ of citric acid), thus avoiding the formation of suspension of polymeric Au(I)−GS complexes. In our case, these Au NCs are co-stabilized by GSH and citrate ligands, which endow the Au NCs bearing good colloidal stability in aqueous solution. As expected, the solution of GS/C−Au NCs is rather stable in water at room temperature. For example, flocculation or precipitation is not noticeable in the solution; their emission spectra also do not change significantly up to 6 months (Fig. S8†).

The fluorescence intensity of GS/C−Au NCs at pH range from 4 to 9 was characterized in detail for their further applications in the human cell. The pH of the aqueous solution of the resulting GS/C−Au NCs is about 5.6, at which their fluorescence intensity is defined as 1. The pH value of their aqueous solution is adjusted by addition of NaOH or HCl solution. When the pH is in the range of 4.1 ~ 8.6, the fluorescence intensity of GS/C−Au NCs increases from 0.5 to 1.5 with pH increase in a fair linear way (Fig. 8). Interestingly, their fluorescence intensity can be recovered when the pH is backwards adjusted to about 5.6 (blue solid square to red solid triangular shapes in Fig. 8). It is plausible that the negatively charge density on the surfaces of GS/C−Au NCs is changed with pH adjustment due to transitions among differently stable states of GSH-citrate complex (Scheme 2). Thus, when the pH decreases from 5.6 to 4.1 (from Scheme 2a to 2b), GS/C−Au NCs start to aggregate due to decrease of electrostatic forces among them and to form spherical agglomerates (Fig. S9†), leading to the decrease in fluorescence intensity. Thanks to the buffer effect of citrate and GS ligands, their aggregation behavior is reversible. These spherical agglomerates of GS/C−Au NCs can be redispersed into single ones by increasing pH from 4.1 to 5.6. Accordingly, their fluorescence intensity are also recovered (b to b' in Fig. 8). When the pH is below 4, the fluorescence intensity of GS/C−Au NCs is too low to meet the requirement of the applications.

When the pH of the aqueous solution of GS/C−Au NCs increases from 5.6 to 8.6, the coordinative structure of GSH and citrate ligands would be like the ones in Scheme 2. Accordingly, the negatively charge density on the surfaces of GS/C−Au NCs would be increased due to the increasingly free carboxylate groups (Scheme 2a to 2c). Accordingly, when the pH is backwards adjusted from 8.6 to 5.6, the negatively charge density on the surfaces of GS/C−Au NCs would be decreased due to transition of citrate to hydrogen citrate ions, thus leading to the recovery of their fluorescence intensity to the initial state (c, d, e and f to c', d', e' and f', respectively, in Fig. 8).

The data from zeta potential analyzer also confirm the changes of their surface charge density. As shown in Fig. 9, their zeta potential values decreases from -22.9 to -31.8, -42.6, -45.5 and -51.2 mV with increase of their pH from 4.1 to 5.6, 6.1, 7.4 and 8.6, respectively. The results also indicate that our solution of GS/C−Au NCs have a good colloidal stability.[51] In our cases, the fluorescence intensity of GS/C−Au NCs increases with increase of the negatively charge density on their surfaces, which is in good agreement with previous work by Goldys.[52] Due to the

strong fluorescence and intensity variation at pH between 4.1 and 8.6 in fair linear way, the Au NCs may be used as intracellular pH meter.[53-55] The work is under way.
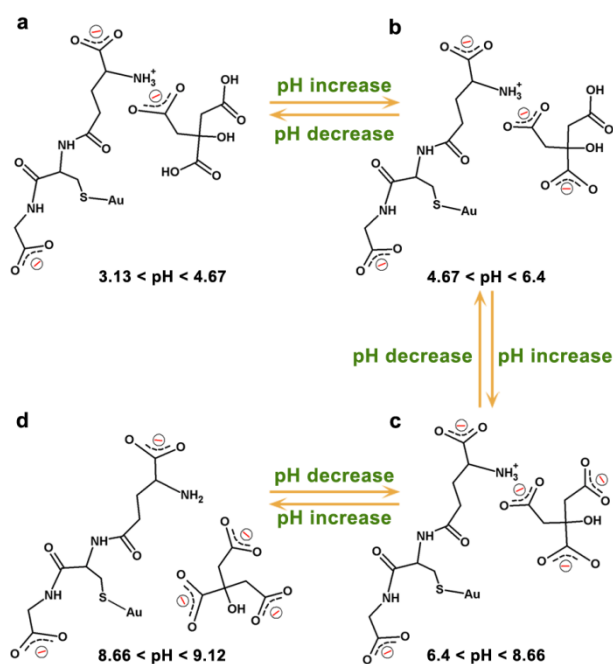


**Scheme 2.** Schematic representation of the coordinative structures of GSH and citrate ligands under different pH ranges.
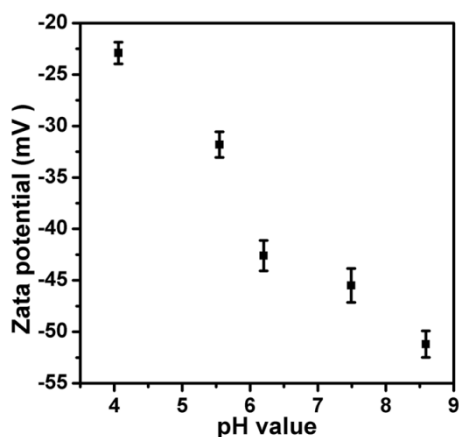


**Fig. 9** Zeta Potential of GS/C−Au NCs solutions measured at different pH values. The error bars represent variations among five separate measurements.

As shown in Scheme 2d, the dissociation between amino groups from GS molecules and carboxylate groups from hydrogen citrate ligands would happen when the pH of the solution is bigger than 8.66 (pKa$_3$ of GSH). Thus, the surface charge density would decrease; their fluorescence intensity would decrease. Further increasing the pH bigger than 9.12 (pKa$_4$ of GSH), the bonds between thiol groups from GS ligands and Au(I) would start to dissociate. These Au(I)···Au(I) non-covalent interactions would be broken.[18] Therefore, some of the deprotonated polymeric Au(I)−GS complexes in the shells would start to decompose and dissolve in water, thus leading to the decrease of their fluorescence intensity. As expected, when the pH is adjusted to bigger than 8.66, fluorescence intensity of GS/C

−Au NCs is decreased gradually. In addition, their fluorescence intensity in the pH range between 8.66 and 9.12 is still stable while their fluorescence intensity at the pH bigger than 9.8 would gradually disappear within 24 h (Fig. S10†). In addition, their fluorescence intensity cannot be recovered even if their pH values are adjusted to initial values. As shown in TEM image (Fig. S11†), larger network-like aggregates of GS/C−Au NCs are formed. It is probably due to the fact that the soluble polymeric Au(I)−GS complexes in water interact with the remaining shells of dispersed GS/C−Au NC to form the networks. Accordingly, their fluorescence intensity of GS/C − Au NCs is gradually decreased due to the gradual decomposition and dissolution of polymeric Au(I)−GS complexes in the shells in water, which is responsible for their strong fluorescence generated by the AIE. Eventually, their fluorescence intensity decreases to nearly zero due to the disappearance of the shells of polymeric Au(I)−GS complexes. The results further confirm that the presence of core-shell structure in the GS/C−Au NCs; the presence of the shells of polymeric Au(I)−GS complexes is the key factor for the strong fluorescence generated by the AIE.
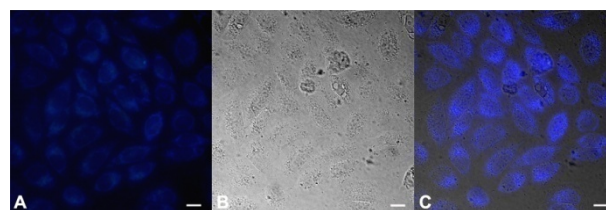
**3.8 Cellular imaging.**



**Fig. 10** Wide-field fluorescence image of HeLa cells (A) after incubation with as-prepared GS/C−Au NCs (200 μg ml$^{-1}$) for 30 min, differential interference contrast (DIC) image, and merged image of A and B (C). $\lambda_{ex}$ = 330-385 nm; $\lambda_{em}$ > 410 nm. Scale bar is 20 μm.

It is known for Au NCs as fluorescent probes for bio-imaging that small size of Au NCs make them easy to penetrate into cells and be able to target the inside portions of the cells. In addition, the Au NCs should have good colloidal stability and higher brightness at the pH of 6 ∼ 8 as the pH of cytoplasm of the cells is about 7.2. The as-prepared fluorescent GS/C−Au NCs have ultrasmall size, high monodispersity, greater brightness and excellent colloidal stability at 7.2, thus they may be a good fluorescent probe for bio-imaging. Fig. 10 shows the images of the HeLa cells incubated with Au NCs (200 μg ml$^{-1}$) for 30 min by using wide-field fluorescence microscopy. The emission intensity from GS/C−Au NCs is collected; strong blue color from the cells is clearly observed (Fig. 10A). However, there is no fluorescence observed from the cells (Fig. S12†) in our control experiment at the same experimental conditions without incubation with the Au NCs. Moreover, the bright fluorescence from GS/C−Au NCs endocytosed by cells are mainly located at the cytoplasm of the cells by merged image (Fig. 10C) of differential interference contrast (DIC) image (Fig. 10B) and fluorescence image (Fig. 10A). The result demonstrates that the observed fluorescence indeed stems from the Au NCs attached to those cells instead of autofluorescence of the cells.

## Conclusions

In summary, we demonstrate a strategy for synthesis of water-

soluble, highly fluorescent Au NCs by co-reduction of GSH and citrate at low temperature (50 °C) within 24 h. The as-prepared GS/C−Au NCs with sizes of about 1.8 nm is highly monodisperse. The GS/C−Au NCs exhibit excitation and emission maximum at 5 385 and 575 nm, respectively; the fluorescence quantum yield is 1.7 %. The high content of Au(I)−thiolate complexes (about 75 %) on the surfaces of core-shell structured GS/C−Au NCs obtained under optimal concentration of GSH and citrate is responsible for their strong fluorescence generated by the AIE. The citrate is 10 used to (i) lower the reaction temperature; (ii) control formation rate of Au(0) cores by selective reduction of Au(III) ions under optimal conditions; and (iii) enhance the colloidal stability of GS/C−Au NCs in the wide pH range from 4.1 to 8.6 due to differently stable states of glutathione-citrate complex. In 15 addition, fluorescence intensity of GS/C−Au NCs obtained is pH-dependent and can be reversibly adjusted in the pH range from 4.1 to 8.6 due to changes in their surface charge density stemming from the transitions among differently stable states of glutathione-citrate complex. The result may present a new way to 20 improve the fluorescence intensity and quantum yield by selecting surface ligands to adjust surface charge density. Our preliminary study also demonstrates that GS/C−Au NCs can be used as fluorescent nanoprobes in bio-imaging.

## Acknowledgements

## Notes and references

*a State Key Laboratory of Crystal Materials, Shandong University, Jinan, 250100, P. R China;*
*Email: hbxia@sdu.edu.cn (H. Xia)*
40 *b Ian Wark Research Institute, University of South Australia, Adelaide, 5095, SA, Australia.*
† Electronic Supplementary Information (ESI) available: [details of any supplementary information available should be included here]. See DOI: 10.1039/b000000x/

45 1 R. C. Jin, *Nanoscale*, 2010, **2**, 343−362.
2 Q. B. Zhang, J. P. Xie, Y. Yu and J. Y. Lee, *Nanoscale*, 2010, **2**, 1962−1975.
3 H. Y. Zhang, Q. Liu, T. Wang, Z. J. Yun, G. L. Li, J. Y. Liu and G. B. Jiang, *Anal. Chim. Acta*, 2013, **770**, 140−146.
50 4 S. Palmal, S. K. Basiruddin, A. R. Maity, S. C. Ray and N. R. Jana, *Chem. Eur. J.*, 2013, **19**, 943−949.
5 X. Yang, L. F. Gan, L. Han, D. Li, J. Wang and E. K. Wang, *Chem. Commun.*, 2013, **49**, 2302−2304.
6 L. Shang, N. Azadfar, F. Stockmar, W. Send, V. Trouillet, M. Bruns, 55 D. Gerthsen and G. U. Nienhaus, *Small*, 2011, **7**, 2614−2620.
7 L. Shang, R. M. Dörlich, S. Brandholt, R. Schneider, V. Trouillet, M. Bruns, D. Gerthsen and G. U. Nienhaus, *Nanoscale*, 2011, **3**, 2009−2014.
8 L. Shang and G. U. Nienhaus, *Biophys. Rev.*, 2012, **4**, 313−322.

60 9 X. D. Xia, Y. F. Long and J. X. Wang, *Anal. Chim. Acta*, 2013, **772**, 81−86.
10 C. Zhou, M. Long, Y. P. Qin, X. K. Sun and J. Zheng, *Angew. Chem.*, 2011, **50**, 3168−3172.
11 H. Lin, L. J. Li, C. Y. Lei, X. H. Xu, Z. Nie, M. L. Guo, Y. Huang 65 and S. Z. Yao, *Biosensors and Bioelectronics*, 2013, **41**, 256−261.
12 L. Polavarapu, M. Manna and Q. Xu, *Nanoscale*, 2011, **3**, 429−434.
13 J. Sun, Y. Yue, P. Wang, H. L. He and Y. D. Jin, *J. Mater. Chem. C*, 2013, **1**, 908−913.
14 J. Sun, J. Zhang and Y. D. Jin, *J. Mater. Chem. C*, 2013, **1**, 138−143.
70 15 R. A. Farrer, F. L. Butterfield, V. W. Chen and J. T. Fourkas, *Nano Lett.*, 2005, **5**, 1139−1142.
16 Y. Negishi, Y. Takasugi, S. Sato, H. Yao, K. Kimura and T. Tsukuda, *J. Am. Chem. Soc.*, 2004, **126**, 6518−6519.
17 C. C. Huang, H. Y. Liao, Y. C. Shiang, Z. H. Lin, Z. Yang and H. T. 75 Chang, *J. Mater. Chem.*, 2009, **19**, 755−759.
18 Z. T. Luo, X. Yuan, Y. Yu, Q. B. Zhang, D. T. Leong, J. Y. Lee and J. P. Xie, *J. Am. Chem. Soc.*, 2012, **134**, 16662−16670.
19 R. P. Briñas, M. H. Hu, L. P. Qian, E. S. Lymar and J. F. Hainfeld, *J. Am. Chem. Soc.*, 2008, **130**, 975−982.
80 20 Y. Negishi, K. Nobusada and T. Tsukuda, *J. Am. Chem. Soc.*, 2005, **127**, 5261−5270.
21 C. Lin, T. Y. Yang, C. H. Lee, S. H. Huang, R. A. Sperling, M. Zanella, J. K. Li, J. L. Shen, H. H. Wang, H. I. Yeh, W. J. Parak and W. H. Chang, *Acs Nano*, 2009, **3**, 395−401.
85 22 Y. Yu, X. Chen, Q. F. Yao, Y. Yu, N. Yan and J. P. Xie, *Chem. Mater.*, 2013, **25**, 946−952.
23 T. Huang and R. W. Murray, *J. Phys. Chem. B*, 2001, **105**, 12498−12502.
24 Y. Y. Yang and S. W. Chen, *Nano Lett.*, 2003, **3**, 75−79.
90 25 T. G. Schaaff and R. L. Whetten, *J. Phys. Chem. B*, 2000, **104**, 2630−2641.
26 C. Zhou, C. Sun, M. X. Yu, Y. P. Qin, J. G. Wang, M. Kim and J. Zheng, *J. Phys. Chem. C*, 2010, **114**, 7727−7732.
27 I. Odriozola, I. Loinaz, J. A. Pomposo and H. J. Grande, *J. Mater.* 95 *Chem.*, 2007, **17**, 4843−4845.
28 H. B. Xia, S. O. Bai, J. Hartmann and D. Y. Wang, *Langmuir*, 2010, **26**, 3585−3589.
29 H. S. Li, H. B. Xia, D. Y. Wang and X. T. Tao, *Langmuir*, 2013, **29**, 5074−5079.
100 30 X. Dong, X. Ji, H. L. Wu, L. Zhao, J. Li and W. S. Yang, *J. Phys. Chem. C*, 2009, **113**, 6573−6576.
31 P. Goulet and R. B. Lennox, *J. Am. Chem. Soc.*, 2010, **132**, 9582−9584.
32 Y. Li, O. Zaluzhna, B. L. Xu, Y. A. Gao, J. M. Modest and Y. J. 105 Tong, *J. Am. Chem. Soc.*, 2011, **133**, 2092−2095.
33 S. R. K. Perala and S. Kumar, *Langmuir*, 2013, **29**, 9863−9873.
34 H. Häkkinen, M. Walter and H. Grönbeck, *J. Phys. Chem. B*, 2006, **110**, 9927−9931.
35 M. S. C. Flett, *Transactions of the Faraday Society*, 1948, **44**, 767− 110 774.
36 A. Barth, *Progress in Biophysics & Molecular Biology*, 2000, **74**, 141–173.
37 H. Muhammed and T. Pradeep, *Chem. Phys. Lett.*, 2007, **449**, 186– 190.
115 38 R. E.Bachman, S. A. Bodolosky-Bettis, S. C. Glennon and S. A. Sirchio, *J. Am. Chem. Soc.*, 2000, **122**, 7146−7147.
39 V. W.-W. Yam and K. Kam-Wing, Lo, *Chem. Soc. Rev.*, 1999, **28**, 323−334.
40 U. Kreibig and M. Vollmer, Optical Properties of Metal Clusters. 120 *Springer Ser. Mat. Sci*, 1995, **25**.
41 H. F. Qian and R. C. Jin, *Nano Lett.*, 2009, **9**, 4083−4087.
42 Y. Levi-Kalisman, P. D. Jadzinsky, N. Kalisman, H. Tsunoyama, T. Tsukuda, D. A. Bushnell and R. D. Kornberg, *J. Am. Chem. Soc.*, 2011, **133**, 2976−2982.
125 43 H. Schmidbaur, *Chem. Soc. Rev.*, 1995, **24**, 391−3400.
44 Z. Assefa, B. G. McBurnett, R. J. Staples, J. P. Fackler, B. Assmann, K. Angermaier and H. Schmidbaur, *Inorg. Chem.*, 1995, **34**, 75−83.
45 H. Ito, T. Saito, N. Oshima, N. Kitamura, S. Ishizaka, Y. Hinatsu, M. Wakeshima, M. Kato, K. Tsuge and M. Sawamura, *J. Am. Chem.* 130 *Soc.*, 2008, **130**, 10044−10045.

46  C. Wang, Y. J. Hu, C. M. Lieber and S. H. Sun, *J. Am. Chem. Soc.*, 2008, **130**, 8902−8903.

47  U. Resch-Genger, M. Grabolle, S. Cavaliere-Jaricot, R. Nitschke and T. Nann, *Nat. Methods*, 2008, **5**, 763−775.

5  48  A. M. Smith and S. Nie, *J. Am. Chem. Soc.*, 2008, **130**, 11278−11279.

49  I. Ojea-Jiménez, N. G. Bastús and V. Puntes, *J. Phys. Chem. C*, 2011, **115**, 15752−15757.

50  X. H. Ji, X. N. Song, J. Li, Y. B. Bai, W. S. Yang and X. G. Peng, *J. Am. Chem. Soc.*, 2007, **129**, 13939−13948.

10  51  A. V. Delgado, F. González-Caballero, R. J. Hunter, L. K. Koopal and J. Lyklema, *J. Colloid Interface Sci.*, 2007, **309**, 194−224.

52  E. M. Goldys and M. A. Sobhan, *Adv. Funct. Mater.*, 2012, **22**, 1906−1913.

53  A. Mooradian, *Phys. Rev. Lett.*, 1969, **22**, 185−187.

15  54  Chin and D. G. Allen, *J. Physiol.*, 1998, **512**, 831−840.

55  J. Y. Han and K. Burgess, *Chem. Rev.*, 2010, **110**, 2709−2728.